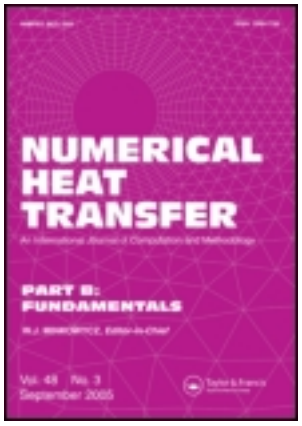

Numerical Heat Transfer, Part B: Fundamentals: An International Journal of Computation and Methodology
Publication details, including instructions for authors and subscription information:
http://www.tandfonline.com/loi/unhb20

On the Accuracy of a Finite-Difference Method for Parabolic Partial Differential Equations with Discontinuous Boundary Conditions

M. Vynnycky [a] & S. L. Mitchell [a]
[a] Mathematics Applications Consortium for Science and Industry (MACSI), Department of Mathematics and Statistics , University of Limerick , Limerick , Ireland

To cite this article: M. Vynnycky & S. L. Mitchell (2013) On the Accuracy of a Finite-Difference Method for Parabolic Partial Differential Equations with Discontinuous Boundary Conditions, Numerical Heat Transfer, Part B: Fundamentals: An International Journal of Computation and Methodology, 64:4, 275-292

To link to this article: http://dx.doi.org/10.1080/10407790.2013.797312

Numerical Heat Transfer, Part B, 64: 275–292, 2013

ISSN: 1040-7790 print/1521-0626 online
DOI: 10.1080/10407790.2013.797312

Taylor & Francis
Taylor & Francis Group

ON THE ACCURACY OF A FINITE-DIFFERENCE METHOD FOR PARABOLIC PARTIAL DIFFERENTIAL EQUATIONS WITH DISCONTINUOUS BOUNDARY CONDITIONS

M. Vynnycky and S. L. Mitchell
Mathematics Applications Consortium for Science and Industry (MACSI), Department of Mathematics and Statistics, University of Limerick, Limerick, Ireland

Although the numerical solution of parabolic partial differential equations (PDEs) is widely documented, the effect of discontinuous boundary conditions on numerical accuracy is not. This article employs the Keller box finite-difference method to study the effect of such discontinuities when solving the linear one-demensional transient heat equation. We demonstrate that this formally second-order-accurate scheme can lose accuracy, but that an analytical understanding of the behavior of the solution helps in providing an accuracy-restoring formulation. Benchmark computations are presented that will provide guidance in the numerical solution of nonlinear parabolic PDEs for which there are no closed-form analytical solutions.

1. INTRODUCTION

Parabolic partial differential equations (PDEs) arise in a wide range of applications in natural science, engineering, and technology; typically, they must be solved numerically and there are, by now, many finite-difference and finite-element schemes in order to do this. While the numerical accuracy of such methods is well established when there are no discontinuities in the boundary conditions, this is often not the case: Examples are the trailing edge of a Blasius boundary layer flow [1–4], the leading and trailing edges of a circular sleeve in a Batchelor flow [5, 6], at the onset of phase change in ablation and the continuous casting of metals [7–9], and in the concentration boundary layer at the edges of electrodes in electrolytic cells [10–12]. In spite of this common occurrence, there appears to be no systematic understanding of the impact of discontinuities on numerical accuracy, nor how it can be alleviated; this is in contrast to the state of the art in problems that have discontinuities in initial conditions, for which analysis is already available [13]. Thus, the purpose of this

Received 10 September 2012; accepted 8 April 2013.
The authors acknowledge the support of the Mathematics Applications Consortium for Science and Industry (MACSI, www.macsi.ul.ie), funded by the Science Foundation Ireland Mathematics Initiative Grant 06/MI/005.
Address correspondence to Sarah L. Mitchell, MACSI, Department of Mathematics and Statistics, University of Limerick, Limerick, Ireland. E-mail: sarah.mitchell@ul.ie

article is to study the numerical solution of test problems that have discontinuous boundary conditions.

Among numerical schemes for the solution of parabolic PDEs, one of the most versatile is the Keller box finite-difference method, and hence we consider it here; in addition to its original application to fixed-boundary problems [14–16], it has recently also been applied extensively to moving-boundary problems [9, 17–19]. Although the scheme is often stated to be formally second-order-accurate in both the streamwise (timelike) and transverse (spacelike) variables, it is only quite recently that the meaning of this statement has been scrutinized more closely. For example, what should be used as the criterion for determining the accuracy of the method is unclear, since the Keller box scheme reformulates an mth-order system for a function F as a system of first-order PDEs—consequently, should one use F or the dependent variable in each of the first-order PDEs? If it is the latter, then F and its space derivatives up to $F^{(m-1)}$ should all be second-order-accurate. Of relevance to this discussion is the observation that early applications of the method were for the steady-state boundary-layer equations that arise in fluid mechanics and heat transfer, for which the governing equations were reformulated in terms of similarity-like variables; subsequently, the PDEs reduced to ordinary differential equations (ODEs) in the limit as the leading edge of the boundary layer is approached. However, although not noted in [14–16], this transformation appears to be crucial for ensuring that the scheme is second-order-accurate for F and its first $(m-1)$ derivatives; without this transformation, more recent computations when $m=2$ indicate that the method is second-order-accurate for F, but of lower accuracy for its first derivative [9, 18]. In fact, more often than not, it will not be possible to commence a numerical integration using a similarity solution, which suggests potential limitations with regard to the accuracy of the method.

A further important point is the distinction between the accuracy of the solution and the accuracy of the scheme [13]. Whereas the accuracy of the scheme can always be determined, the accuracy of the solution can only be found if there is an analytical solution against which the numerical solution can be compared; consequently, in the majority of cases, it is not possible to determine the accuracy of the solution and, furthermore, nor is it possible to infer it from the accuracy of the scheme. Thus, it is hoped that the results of this article can then serve as a benchmark for problems that have discontinuous boundary conditions but do not have analytical solutions; consequently, the focus here is problems with analytical solutions.

The simplest example of the more general situation that we wish to consider is given by the linear 1-D transient heat equation,

$$\frac{\partial T}{\partial t} = \frac{\partial^2 T}{\partial x^2} \quad \text{for } 0 < x < \infty \tag{1}$$

subject to the initial condition

$$T = f(x) \quad \text{at } t = 0 \tag{2}$$

and the boundary conditions

$$T = g_1(t) \quad \text{at } x = 0 \tag{3}$$

or

$$\frac{\partial T}{\partial x} = g_2(t) \quad \text{at } x = 0 \tag{4}$$

and

$$T \to f(\infty) \quad \text{as } x \to \infty \tag{5}$$

where $f(\infty)$ is taken to be finite. Although there is no evident discontinuity in the boundary condition at $x = 0$, the implication is that Eq. (1) has been integrated up to $t = 0$ subject to some boundary condition at $x = 0$ which gives rise to $T = f(x)$ at $t = 0$, and is then considered as the initial condition for the problem for $t > 0$. In the remainder of this article, we shall look in turn at solutions to Eq. (1), subject to (2), (5), and

A. Equation (3), with $f(0) \neq g_1(0)$

B. Equation (3), with $f(0) = g_1(0)$

C. Equation (4), with $f'(0) \neq g_2(0)$, where $'$ denotes differentiation with respect to x

D. Equation (4), $f'(0) = g_2(0)$

The layout of the article is as follows. In Section 2 we present analysis related to these four cases, whereas in Section 3 we give details of the numerical implementation. In Section 4 we show the results, and conclusions are drawn in Section 5.

2. ANALYTICAL SOLUTIONS

2.1. Case A

In this case, we use boundary equation (3) and we suppose that $f(0) \neq g_1(0)$; it is clear that T is inconsistent at (0, 0), in the sense that

$$\lim_{t \to 0} T(0, t) \neq \lim_{x \to 0} T(x, 0)$$

As highlighted in [9], an inconsistency of this sort leads to a loss of numerical accuracy if an attempt is made to solve the equations (1)–(3) and (5) as they stand; we define formally what is meant by "accuracy" in Section 3. To avoid this loss of accuracy, we set

$$T(x, t) = g_1(0) + [f(0) - g_1(0)]\text{erf}\left(\frac{x}{2\sqrt{t}}\right) + \mathcal{T}(x, t) \tag{6}$$

which leads to

$$\frac{\partial^2 \mathcal{T}}{\partial x^2} = \frac{\partial \mathcal{T}}{\partial t} \quad \text{for } 0 < x < \infty \tag{7}$$

subject to

$$\mathcal{T} = g_1(t) - g_1(0) \quad \text{at } x = 0 \tag{8}$$

$$\mathcal{T} \to f(\infty) - f(0) \quad \text{as } x \to \infty \tag{9}$$

$$\mathcal{T} = f(x) - f(0) \quad \text{at } t = 0 \tag{10}$$

So, $\mathcal{T}$ is consistent at (0, 0), since

$$\lim_{t\to 0} \mathcal{T}(0,t) = \lim_{x\to 0} \mathcal{T}(x,0) = 0$$

but $\mathcal{T}_x$ might not be; this situation is considered next.

2.2. Case B

For this case, we consider, as a convenient example,

$$f(x) := -1 + e^{-ax} \quad g_1(t) := 0 \tag{11}$$

so that $f(0) = g_1(0)$; this has been chosen because it is relatively straightforward to construct a closed-form expression for T:

$$T(x,t) = -\operatorname{erf}\left(\frac{x}{2\sqrt{t}}\right) + \frac{1}{2}e^{a(-x+at)}\operatorname{erfc}\left(\frac{2at-x}{2\sqrt{t}}\right) - \frac{1}{2}e^{a(x+at)}\operatorname{erfc}\left(\frac{2at+x}{2\sqrt{t}}\right) \tag{12}$$

From (11), we know that T is consistent at (0, 0), whereas from (12),

$$T_x(x,t) = -\frac{a}{2}e^{a(-x+at)}\operatorname{erfc}\left(\frac{2at-x}{2\sqrt{t}}\right) - \frac{a}{2}e^{a(x+at)}\operatorname{erfc}\left(\frac{2at+x}{2\sqrt{t}}\right) \tag{13}$$

so that

$$T_x(0,t) = -a\,e^{a^2 t}\operatorname{erfc}\left(a\sqrt{t}\right) \tag{14}$$

Also, we have $T_x(x, 0) = -ae^{-ax}$; thus, T_x is also consistent at (0, 0), since

$$\lim_{t\to 0} T_x(0,t) = \lim_{x\to 0} T_x(x,0) = -a \tag{15}$$

For the case when both T and T_x are consistent, Mitchell and Vynnycky [9] found that integrating a corresponding system of equations with x and t as the independent variables would give second-order accuracy for T, but not for T_x. In addition to introducing a similarity variable, it turned out to be necessary to reformulate the problem into one that *did* have an inconsistency. This is easily done by simply differentiating the governing equations with respect to x, and introducing $F := \partial T/\partial x$ as the dependent variable. The resulting equations are

$$\frac{\partial^2 F}{\partial x^2} = \frac{\partial F}{\partial t} \quad \text{for } 0 < x < \infty \tag{16}$$

subject to

$$\frac{\partial F}{\partial x} = 0 \quad \text{at } x = 0 \tag{17}$$

$$F \to 0 \quad \text{as } x \to \infty \tag{18}$$

$$F = -ae^{-ax} \quad \text{at } t = 0 \tag{19}$$

which has the exact solution given in (13); note that (17) is arrived at by differentiating (3) with respect to t and then using Eq. (1). From initial condition (19) it follows that $F_x(x, 0) = a^2 e^{-ax}$ and so F_x is inconsistent at (0, 0) as required, since

$$\lim_{t \to 0} F_x(0, t) = 0 \quad \lim_{x \to 0} F_x(x, 0) = a^2 \tag{20}$$

Tied in with introducing an inconsistency is the use of a variable transformation,

$$\eta = \frac{x}{\sqrt{t}} \quad \tau = \sqrt{t} \tag{21}$$

in order to achieve second-order accuracy for both the scheme and the solution, for both F and F_x. In the case of constant initial conditions, it is possible to find a self-starting similarity solution in the limit as $\tau \to 0$; here, however, the initial conditions are not constant, and this constitutes the next level of complication. In general, the solution for $\tau > 0$ develops a double-deck structure [2, 5]: In the lower deck, where $x \sim \tau$, there is a self-starting similarity solution; in the upper deck, where $x \sim O(1)$, the solution evolves from the initial condition, although the two decks must match to each other. The numerical implementation given in [2, 5] results in nonuniform meshes, which would render it impossible to calculate the accuracy of the scheme and the solution; however, Mitchell and Vynnycky [9] found that this difficulty could be avoided by subtracting off the initial condition and defining a new dependent variable. In the present context, we set $F(x, t) = -ae^{-ax} + G(x, t)$, which leads to

$$\frac{\partial^2 G}{\partial x^2} = \frac{\partial G}{\partial t} + a^3 e^{-ax} \quad \text{for } 0 < x < \infty \tag{22}$$

subject to

$$\frac{\partial G}{\partial x} = -a^2 \quad \text{at } x = 0 \tag{23}$$

$$G \to 0 \quad \text{as } x \to \infty \tag{24}$$

$$G = 0 \quad \text{at } t = 0 \tag{25}$$

Finally, using substitution (21) and $G(x, t) = \tau H(\eta, \tau)$, we obtain

$$\frac{\partial^2 H}{\partial \eta^2} = \frac{1}{2} H + \frac{\tau}{2}\frac{\partial H}{\partial \tau} - \frac{\eta}{2}\frac{\partial H}{\partial \eta} + a^3 \tau e^{-a\tau\eta} \quad \text{for } 0 < \eta < \infty \tag{26}$$

subject to

$$\frac{\partial H}{\partial \eta} = -a^2 \quad \text{at } \eta = 0 \tag{27}$$

$$H \to 0 \quad \text{as } \eta \to \infty \tag{28}$$

Now, in the limit as $\tau \to 0$, the system (26)–(28) becomes

$$\frac{d^2 H}{d\eta^2} = \frac{1}{2} H - \frac{1}{2}\eta \frac{dH}{d\eta} \tag{29}$$

subject to

$$\frac{dH}{d\eta} = -a^2 \quad \text{at } \eta = 0 \tag{30}$$

$$H \to 0 \quad \text{as } \eta \to \infty \tag{31}$$

which can be solved to give

$$H(\eta) = a^2 \left[\frac{2}{\sqrt{\pi}} e^{-\eta^2/4} - \eta \operatorname{erfc}\left(\frac{\eta}{2}\right) \right] \tag{32}$$

this serves as the initial condition for (26).

2.3. Case C

Consider now the situation where boundary condition (4) is used and $f'(0) \neq g_2(0)$; thus, T_x is not consistent at (0,0), since

$$\lim_{t \to 0} T_x(0, t) \neq \lim_{x \to 0} T_x(x, 0) \tag{33}$$

Furthermore, without local analysis on a case-by-case basis, it is not clear whether or not T is consistent at (0, 0); for the problems considered in [9, 18, 19], T was consistent. As a particular example which is different to those in [9, 18, 19], we will consider the case when

$$f(x) := -1 + e^{-ax} \quad g_2(t) := -b \tag{34}$$

where a and b are real constants such that $a \neq b$ and with $b \neq 0$. This gives the exact solution

$$T(x,t) = -1 - bx\,\mathrm{erfc}\left(\frac{x}{2\sqrt{t}}\right) + 2b\sqrt{\frac{t}{\pi}}\exp\left(-\frac{x^2}{4t}\right) + \frac{1}{2}e^{a(-x+at)}\,\mathrm{erfc}\left(\frac{2at-x}{2\sqrt{t}}\right) + \frac{1}{2}e^{a(x+at)}\,\mathrm{erfc}\left(\frac{2at+x}{2\sqrt{t}}\right) \tag{35}$$

and so

$$T(0,t) = -1 + 2b\sqrt{\frac{t}{\pi}} + e^{a^2t}\,\mathrm{erfc}\left(a\sqrt{t}\right) \tag{36}$$

indicating that T is consistent at (0, 0), since

$$\lim_{t\to 0} T(0,t) = \lim_{x\to 0} T(x,0) = 0 \tag{37}$$

The resulting problem for T can now be handled in the same way as that for F in case B. We set

$$T(x,t) = f(x) + G(x,t) \tag{38}$$

which then, with f as given in Eq. (34), yields

$$\frac{\partial^2 G}{\partial x^2} = \frac{\partial G}{\partial t} - a^2 e^{-ax} \quad \text{for } 0 < x < \infty \tag{39}$$

subject to

$$\frac{\partial G}{\partial x} = a - b \quad \text{at } x = 0 \tag{40}$$

$$G \to 0 \quad \text{as } x \to \infty \tag{41}$$

$$G = 0 \quad \text{at } t = 0 \tag{42}$$

Finally, using Eq. (21) and setting $G(x, t) = \tau H(\eta, \tau)$, we arrive at

$$\frac{\partial^2 H}{\partial \eta^2} = \frac{1}{2}H + \frac{\tau}{2}\frac{\partial H}{\partial \tau} - \frac{\eta}{2}\frac{\partial H}{\partial \eta} - a^2\tau e^{-a\tau\eta} \quad \text{for } 0 < \eta < \infty \tag{43}$$

subject to

$$\frac{\partial H}{\partial \eta} = a - b \quad \text{at } \eta = 0 \tag{44}$$

$$H \to 0 \quad \text{as } \eta \to \infty \tag{45}$$

Now, in the limit as $\tau \to 0$, the system (43)–(45) becomes

$$\frac{d^2 H}{d\eta^2} = \frac{1}{2}H - \frac{1}{2}\eta\frac{dH}{d\eta} \tag{46}$$

subject to

$$\frac{dH}{d\eta} = a - b \quad \text{at } \eta = 0 \tag{47}$$

$$H \to 0 \quad \text{as } \eta \to \infty \tag{48}$$

which can be solved to give

$$H(\eta) = -(a-b)\left[\frac{2}{\sqrt{\pi}} e^{-\eta^2/4} - \eta \operatorname{erfc}\left(\frac{\eta}{2}\right)\right] \tag{49}$$

This is the initial condition for the system (43)–(45).

2.4. Case D

This time, we have $f'(0) = g_2(0)$, i.e., $a = b$, so that T_x is consistent at (0, 0); in fact, the exact solution is given by Eq. (35) with $a = b$, which indicates that T will also be consistent at (0, 0). Thus, with T and T_x both consistent, we again introduce $F = \partial T/\partial x$ as the dependent variable. Then,

$$\frac{\partial^2 F}{\partial x^2} = \frac{\partial F}{\partial t} \quad \text{for } 0 < x < \infty \tag{50}$$

subject to

$$F = -a \quad \text{at } x = 0 \tag{51}$$

$$F \to 0 \quad \text{as } x \to \infty \tag{52}$$

$$F = -ae^{-ax} \quad \text{at } t = 0 \tag{53}$$

which has the exact solution

$$F(x,t) = \frac{a}{2}\left[e^{a(x+at)} \operatorname{erfc}\left(\frac{2at + x}{2\sqrt{t}}\right) - e^{a(-x+at)} \operatorname{erfc}\left(\frac{2at - x}{2\sqrt{t}}\right) - 2\operatorname{erfc}\left(\frac{x}{2\sqrt{t}}\right)\right]. \tag{54}$$

Now, F is consistent, but F_x is not, so the situation is not entirely identical to that in case B. With $\hat{F} := \partial F/\partial x$, the system (50)–(53) becomes

$$\frac{\partial^2 \hat{F}}{\partial x^2} = \frac{\partial \hat{F}}{\partial t} \quad \text{for } 0 < x < \infty \tag{55}$$

subject to

$$\frac{\partial \hat{F}}{\partial x} = -0 \quad \text{at } x = 0 \tag{56}$$

$$\hat{F} \to 0 \quad \text{as } x \to \infty \tag{57}$$

$$\hat{F} = a^2 e^{-ax} \quad \text{at } t = 0 \tag{58}$$

Then, by setting $G(x,t) = a^2 e^{-ax} + \hat{F}(x,t)$, we have

$$\frac{\partial^2 G}{\partial x^2} = \frac{\partial G}{\partial t} + a^4 e^{-ax} \quad \text{for } 0 < x < \infty \tag{59}$$

subject to

$$\frac{\partial G}{\partial x} = -a^3 \quad \text{at } x = 0 \tag{60}$$

$$G \to 0 \quad \text{as } x \to \infty \tag{61}$$

$$G = 0 \quad \text{at } t = 0 \tag{62}$$

Finally, we use the substitution (21) and $G(x, t) = \tau H(\eta, \tau)$ to obtain

$$\frac{\partial^2 H}{\partial \eta^2} = \frac{1}{2} H + \frac{\tau}{2}\frac{\partial H}{\partial \tau} - \frac{\eta}{2}\frac{\partial H}{\partial \eta} + a^4 \tau e^{-a\tau\eta} \quad \text{for } 0 < \eta < \infty \tag{63}$$

subject to

$$\frac{\partial H}{\partial \eta} = -a^3 \quad \text{at } \eta = 0 \tag{64}$$

$$H \to 0 \quad \text{as } \eta \to \infty \tag{65}$$

Now, in the limit as $\tau \to 0$, the system (63)–(65) becomes

$$\frac{d^2 H}{d\eta^2} = \frac{1}{2} H - \frac{1}{2}\eta \frac{dH}{d\eta} \tag{66}$$

subject to

$$\frac{dH}{d\eta} = -a^3 \quad \text{at } \eta = 0 \tag{67}$$

$$H \to 0 \quad \text{as } \eta \to \infty \tag{68}$$

and this can be solved to give

$$H(\eta) = a^3 \left[\frac{2}{\sqrt{\pi}} e^{-\eta^2/4} - \eta \operatorname{erfc}\left(\frac{\eta}{2}\right) \right] \tag{69}$$

which becomes the initial condition for (63)–(65).

3. NUMERICAL IMPLEMENTATION

3.1. Discretization

In essence, the numerical task that remains is to solve the three systems of equations (26)–(28), (43)–(45) and (63)–(65), subject to initial conditions (32), (49), and (69), respectively. Clearly, they are qualitatively very similar, so we address directly only one of these; we choose (26)–(28) and (32). More particularly, the task is to demonstrate that both the numerical scheme and the solution are second-order-accurate for H and H_η. In addition, we will also wish to investigate the effect on numerical accuracy of *not* taking adequate account of discontinuities; to this end, we will compute solutions to Eqs. (22)–(25) and (50)–(53) also, as these give numerical accuracy for the dependent variable and its first spatial derivative that is different to that for H and H_η.

First, we explain the application of the Keller box scheme to Eqs. (26)–(28) and (32); for Eqs (22)–(25) and (50)–(53), the procedure is similar. It is convenient to rewrite (26) as a system of two first-order equations by setting $V = \partial H/\partial\eta$. This gives

$$H_\eta = V \tag{70}$$

$$V_\eta = \frac{1}{2}H + \frac{\tau}{2}H_\tau - \frac{\eta}{2}V + a^3\tau e^{-a\tau\eta} \tag{71}$$

with boundary conditions

$$V = -a^2 \quad \text{at } \eta = 0 \tag{72}$$

$$H \to 0 \quad \text{as } \eta \to \infty \tag{73}$$

and initial conditions

$$H(\eta,0) = a^2\left[\frac{2}{\sqrt{\pi}}e^{-\eta^2/4} - \eta\,\mathrm{erfc}\left(\frac{\eta}{2}\right)\right] \quad V(\eta,0) = -a^2\mathrm{erfc}\left(\frac{\eta}{2}\right) \tag{74}$$

For a variable χ and independent variables τ and η, we define the following finite-difference operators:

$$\mu_\tau\chi_{i+1/2}^{n+1/2} = \frac{\chi_{i+1/2}^{n+1} + \chi_{i+1/2}^{n}}{2} \quad \delta_\tau\chi_{i+1/2}^{n+1/2} = \frac{\chi_{i+1/2}^{n+1} - \chi_{i+1/2}^{n}}{\Delta\tau} \tag{75}$$

$$\mu_\eta\chi_{i+1/2}^{n+1/2} = \frac{\chi_{i+1}^{n+1/2} + \chi_{i}^{n+1/2}}{2} \quad \delta_\eta\chi_{i+1/2}^{n+1/2} = \frac{\chi_{i+1}^{n+1/2} - \chi_{i}^{n+1/2}}{\Delta\eta} \tag{76}$$

where $\Delta\eta$ and $\Delta\tau$ are the uniform mesh spacings in the η and τ directions, respectively, and n and i are their respective indices. The box scheme applied to Eqs. (70) and (71) therefore gives, for $n = 0, 1, 2, \ldots$, and with $I + 1$ mesh points in η,

$$\mu_\tau\delta_\eta H_{i+1/2}^{n+1/2} = \mu_\tau\mu_\eta V_{i+1/2}^{n+1/2}, \tag{77}$$

$$\mu_\tau\delta_\eta V_{i+1/2}^{n+1/2} = \frac{1}{2}\mu_\eta\delta_\tau\left(\tau_{n+1/2}H_{i+1/2}^{n+1/2}\right) + \mu_\tau\mu_\eta\left(\frac{1}{2}H_{i+1/2}^{n+1/2} - \frac{1}{2}\eta_{i+1/2}V_{i+1/2}^{n+1/2} + a^3\tau_{n+1/2}e^{-a\tau_{n+1/2}\eta_{i+1/2}}\right) \quad (78)$$

which holds for $i = 1, \ldots, I-1$; note that (78) gives rise to a parameter, $\nu := \Delta\tau/\Delta\eta$. Boundary conditions (72) and (73) are

$$V_0^n = -a^2 \quad (79)$$

$$H_I^n = 0 \quad (80)$$

respectively. From (74), the initial conditions are written as

$$H_i^0 = a^2\left[\frac{2}{\sqrt{\pi}}e^{-\eta_i^2/4} - \eta_i\,\mathrm{erfc}\left(\frac{\eta_i}{2}\right)\right] \quad V_i^0 = -a^2\mathrm{erfc}\left(\frac{\eta_i}{2}\right) \quad (81)$$

3.2. Order of Accuracy

We will also wish to determine the order of accuracy of the scheme and of the solution. We start this discussion by considering a sequence $\Delta\eta_k$ where

$$\Delta\eta_k = 2^{-k}\Delta\eta_0 \quad k = 1, 2, \cdots$$

and we denote the space coordinates of meshes associated with this sequence by

$$\eta_{i,k} = i\Delta\eta_k \quad i = 0, 1, \cdots, I_k \quad k = 0, 1, 2, \cdots$$

where

$$I_k = 2^k I_0 \quad k = 1, 2, \cdots.$$

As discussed in [13], for a general numerical solution $H_{2^k i}^n$ and corresponding exact solution $h(\eta_{i,\,k}, \tau^n)$ at the nth time step, τ^n, the error and corresponding order of convergence, $E_{H,k}^n$ and $p_{H,k}$, respectively, are given by

$$E_{H,k}^n = \left\{\Delta\eta_k\sum_{i=0}^{I_0}\left[h(\eta_{i,0}, \tau^n) - H_{2^k i}^n\right]^2\right\}^{1/2} \quad p_{H,k} = \frac{\ln(E_{H,k}^n/E_{H,k+1}^n)}{\ln 2} \quad (82)$$

for $k = 0, 1, 2, \ldots$; furthermore, the accuracy of the solution with respect to H, p_H, is then

$$p_H = \lim_{k\to\infty} p_{H,k} \quad (83)$$

As for the accuracy of the scheme with respect to H, $\bar{p}_H$, we first define

$$\overline{E}_{H,k}^n = \left[\sum_{i=0}^{I_0}\left(H_{2^k i}^n - H_{2^{k-1} i}^n\right)^2\right]^{1/2} \quad \bar{p}_{H,k} = \frac{\ln(\overline{E}_{H,k}^n/\overline{E}_{H,k+1}^n)}{\ln 2} \quad (84)$$

for $k = 1, 2, \ldots$; then

$$\bar{p}_H = \lim_{k \to \infty} \bar{p}_{H,k} \tag{85}$$

In cases where an exact solution was known and there were no discontinuities in the boundary conditions after reformulation, Mitchell and Vynnycky [17] showed that $p_H = \bar{p}_H$. Furthermore, Mitchell et al. [18] demonstrated that it was also possible to apply this idea to the spatial derivative of H; thus, we set, for $k = 0, 1, 2, \ldots$,

$$E^n_{V,k} = \left\{ \Delta\eta_k \sum_{i=0}^{I_0} \left[v(\eta_{i,0}, \tau^n) - V^n_{2^k i} \right]^2 \right\}^{1/2} \quad p_{V,k} = \frac{\ln(E^n_{V,k}/E^n_{V,k+1})}{\ln 2} \tag{86}$$

where $v = \partial h / \partial \eta$, and

$$\overline{E}^n_{V,k} = \left[\sum_{i=0}^{I_0} \left(V^n_{2^k i} - V^n_{2^{k-1} i} \right)^2 \right]^{1/2} \quad \bar{p}_{V,k} = \frac{\ln(\overline{E}^n_{V,k}/\overline{E}^n_{V,k+1})}{\ln 2} \tag{87}$$

for $k = 1, 2, \ldots$.

3.3. Further Considerations

The fact that f is not constant, which manifests itself as the fourth term—call it f^*—on the right-hand side of Eq. (71), leads to several interrelated numerical issues that must be treated. First of all, although it is clear that, in practice, a finite computational domain of extent η_∞ is chosen, considerably greater care must be taken regarding this choice than in earlier work in order to ensure that the correct asymptotic behavior is captured as $\eta \to \infty$. When f is constant, so that $f^* = 0$, then, since H is known to decay exponentially as $\eta \to \infty$, $\eta_\infty = 10$ proves to be large enough. However, when $f^* \neq 0$, it is necessary to know how it decays as $x \to \infty$, since this decay must be correctly reflected in the discretized version of Eq. (71); for reference, this is shown for $\exp(-ax)$ for $a = 1$ and 4 in Figure 1. Since $x = \eta\tau$, this means that if the value of η_∞ is too small, then the asymptotic decay of f^* will not be captured in the numerical solution; so, it appears, at first sight, necessary to take

$$\eta_\infty \Delta\tau \gg 1/a \tag{88}$$

However, the process of determining the accuracy, as described in [13] and applied below, relies on decreasing the value of $\Delta\tau$, and it is evident that as k increases, inequality (88) will no longer be satisfied, no matter how large we take η_∞. In fact, there turns out to be a neat resolution to this particular issue. Because the accuracy check requires that solutions be computed numerically for meshes that have different $\Delta\eta$, it does not require η_∞ be the same for each refinement; consequently, if we double η_∞ and increase I fourfold, then we will simultaneously halve the size of $\Delta\eta$—exactly what is necessary when performing accuracy checks for problems posed on finite domains.

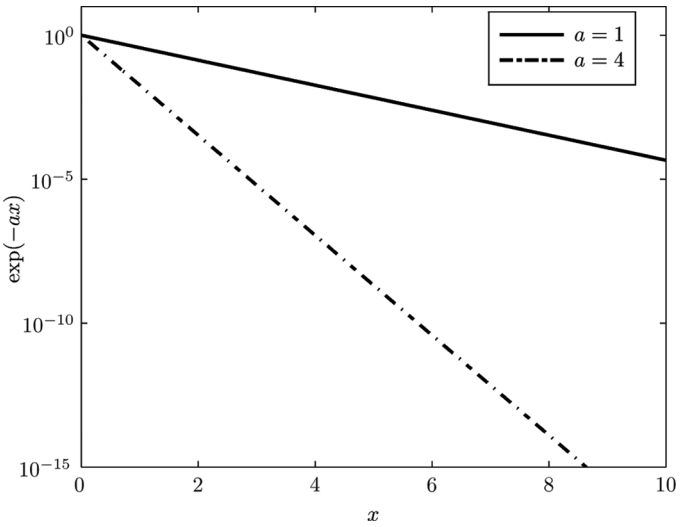

Figure 1. $\exp(-ax)$ versus x for $a = 1$ and 4.

On a more general note, e.g., in ablation and continuous casting, an analytical expression for $f^*(x)$ will not exist; it will typically have been computed following numerical integration up to $t = 0$. This leads to a dilemma as to what to use for $f^*(x)$, or rather $f^*(\eta\tau)$, in Eq. (71), since $f^*(\tau_n\eta_i)$ will not have been computed for all the values of τ_n and η_i at which it is required. One of the appealing features of the double-deck schemes in [2, 5] was that this issue was resolved simply by dropping points systematically from the upper deck; thus, there was no need to introduce new arbitrary points. Here, we adopt a different approach: When f^* is required at (τ_n, η_i), we interpolate the value of $f^*(\tau_n\eta_i)$ from $(f_I^*)_{i=0,\cdots,I}$ if $\tau_n\eta_i < x_I$; otherwise, if $\tau_n\eta_i \geq x_I$, we set $f^*(\tau_n\eta_i) = f_I^*$. As we will show in Section 4, this turns out to have no adverse effects on either the accuracy of the scheme or the accuracy of the solution.

4. RESULTS

We present first results for the formulations that do not give optimal accuracy, i.e., Eqs. (22)–(25) and (50)–(53); then, we will present the results for the formulation which ultimately does, i.e., Eqs. (26)–(28) and (32).

Table 1 shows results from solving (22)–(25) for two different values of a; in these runs, the outer edge of the computational domain, x_∞, was set at 10. It is evident that p and $\bar{p}$ for both U and G seem to be converging toward 1, although the trend is slower for the higher value of a.

Table 2 shows results from solving (50)–(53) for the same values of a and x_∞. This case gives different, and seemingly more ambiguous, convergence behavior to the first one. First of all, there is strong evidence that the accuracy of the numerical scheme for the temperature-like variable, $\bar{p}_F$, is 2, but that for the heat flux–like variable, $\bar{p}_W$, is just 1. The corresponding accuracies for the solution, p_F and p_W, give considerably less meaningful values, however. In view of the inferior accuracy of

Table 1. Comparison of the order of accuracy of the numerical solution of (22)–(25) for G and U at fixed $t^n = 1$ with $\Delta t/\Delta x = 1$

	$x_\infty = 10,\ a = 1$				$x_\infty = 10,\ a = 4$			
Δx (k)	p_G	$\bar{p}_G$	p_U	$\bar{p}_U$	p_G	$\bar{p}_G$	p_U	$\bar{p}_U$
1/10 ($k = 1$)	1.08553		1.15753		1.35882		1.54780	
1/20 ($k = 2$)	1.03863	1.09413	1.07852	1.41818	1.20543	1.43436	1.31969	1.80477
1/40 ($k = 3$)	1.01979	1.04079	1.03900	1.09960	1.11318	1.26668	1.17703	1.43299
1/80 ($k = 4$)	1.00995	1.01601	1.01893	1.03966	1.05954	1.14812	1.09208	1.22954

Table 2. Comparison of the order of accuracy of the numerical solution of (50)–(53) for F and $W = \partial F/\partial x$ at fixed $t^n = 1$ with $\Delta t/\Delta x = 1$

	$x_\infty = 10,\ a = 1$				$x_\infty = 10,\ a = 4$			
Δx (k)	p_F	$\bar{p}_F$	p_W	$\bar{p}_W$	p_F	$\bar{p}_F$	p_W	$\bar{p}_W$
1/10 ($k = 1$)	2.14940		1.53377		2.25041		1.47112	
1/20 ($k = 2$)	1.74570	2.48805	1.50252	2.65619	2.39787	3.37548	1.50599	2.57860
1/40 ($k = 3$)	0.58246	2.08928	1.49878	1.04406	2.41624	3.10736	1.51051	1.04217
1/80 ($k = 4$)	0.06116	2.00999	1.47477	1.01630	2.37817	2.09754	1.50724	1.04987

these two formulations, we have not investigated them exhaustively, although it should be noted that caution is necessary in interpreting the values of the accuracy indices. Tables 1 and 2 are for when $t = 1$, but it is evident that different p values would have been obtained had we computed them for a different value of t. This is because of the way that the analytical solutions that are used to compute p—Eqs. (13) and (54)—evolve with time; an indication of this is given in Figure 2 for $a = 1$ at

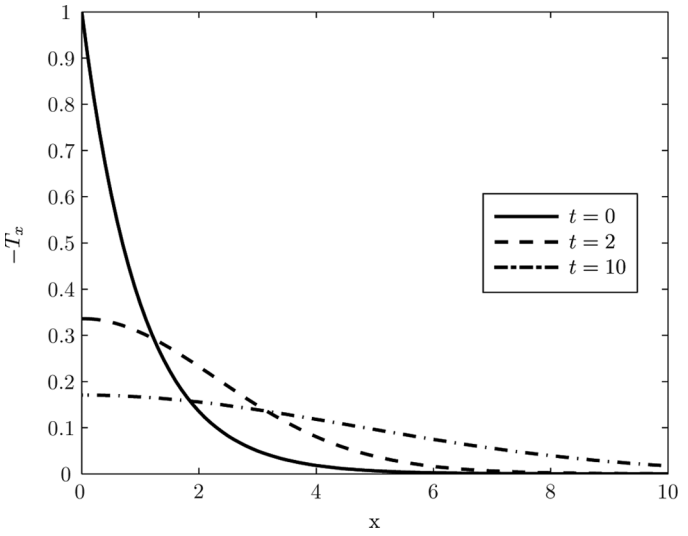

Figure 2. $-T_x$ in Eq. (13) versus x for $a = 1$ at $t = 0$, 2, 10.

Table 3. Comparison of the order of accuracy of the numerical solution of (26)–(28) and (32) for H and V at fixed $\tau^n = 1$ with $\nu = \Delta\tau/\Delta\eta = 1$

	$\eta_\infty = 12$, $a = 1$				$\eta_\infty = 12$, $a = 4$			
$\Delta\eta$ (k)	p_H	$\bar{p}_H$	p_V	$\bar{p}_V$	p_H	$\bar{p}_H$	p_V	$\bar{p}_V$
1/10 ($k=1$)	0.21332		0.49040		2.04095		2.08669	
1/20 ($k=2$)	−0.01625	2.82159	−0.10902	2.80811	2.35423	1.91969	2.04710	2.10217
1/40 ($k=3$)	−0.00657	2.22402	−0.02379	2.22724	1.71432	1.87826	2.14861	1.96274
1/80 ($k=4$)	−0.00149	2.04155	−0.00580	2.04160	−0.74366	1.94500	0.80525	1.98353

Table 4. Comparison of the order of accuracy of the numerical solution of (26)–(28) and (32), with $a = 4$, for H and V at fixed $\tau^n = 0.5$

	$\eta_\infty = 100$, $\nu = 0.5$				$\eta_\infty = 100$, $\nu = 0.1$			
$\Delta\eta$ (k)	p_H	$\bar{p}_H$	p_V	$\bar{p}_V$	p_H	$\bar{p}_H$	p_V	$\bar{p}_V$
1/10 ($k=1$)	−0.70686		1.58268		2.01658		2.35928	
1/20 ($k=2$)	4.74083	1.92492	2.97822	2.63686	2.05199	1.99328	2.00252	2.46621
1/40 ($k=3$)	1.74233	1.84272	2.05073	2.07418	2.24780	1.99135	2.02794	1.99338
1/80 ($k=4$)	0.53586	1.27576	1.93384	2.05154	2.80663	1.99418	2.07957	1.99691

$t = 0, 2, 10$. On the other hand, the computational domain extends only as far as $x = 10$, at which boundary conditions (24) and (52) are prescribed; eventually, for large enough values of t, an error will arise because of this. Consequently, it is better to avoid this problem by solving in transformed variables, to which we turn next.

Table 3 shows results from solving (26)–(28) and (32) for $\eta_\infty = 12$ for the same values of a as in Tables 1 and 2. Observe here that here $\bar{p}$ appears to be tending to 2 for both H and V, although p does not. On considering whether (88) is being satisfied, it is clear that it is not, since even when $\Delta\eta = 1/80$ we have $a\eta_\infty\Delta\tau = 0.6$. In Table 4, we have increased the value of η_∞ considerably and have experimented with the value of ν for the case when $a = 4$; $\bar{p}$ behaves as desired for the lower value of ν, although once again there is concern with regard to the behavior of p.

Lastly, we decided to test the convergence by doubling η_∞ on each iteration; the results are shown in Table 5 for $\nu = 1/4$ and $\nu = 1/6$ and with $a = 4$. Here, we find that p and $\bar{p}$ both converge to 2 for both the temperature-like and heat flux–like

Table 5. Comparison of the order of accuracy of the numerical solution of (26)–(28) and (32), with $a = 4$, for H and V at fixed $\tau^n = 0.5$

		$\nu = 0.25$				$\nu = 0.1667$			
$\Delta\eta$ (k)	η_∞	p_H	$\bar{p}_H$	p_V	$\bar{p}_V$	p_H	$\bar{p}_H$	p_V	$\bar{p}_V$
1/10 ($k=1$)	24	2.00382		2.02516		2.00447		2.36676	
1/20 ($k=2$)	48	2.00154	1.99988	2.01556	2.02921	2.00390	1.99690	2.00771	2.47509
1/40 ($k=3$)	96	1.99926	1.99810	2.01304	2.01646	2.00189	1.99872	2.00580	2.00840
1/80 ($k=4$)	192	1.99780	1.99740	2.01236	2.01328	2.00051	1.99906	2.00531	2.00597

Table 6. Comparison of the order of accuracy of the numerical solution of (26)–(28) and (32) using interpolation for f with $a=4$, for H and V at fixed $\tau^n=0.5$

		$\nu=0.1667$			
$\Delta\eta$ (k)	η_∞	p_H	$\bar{p}_H$	p_V	$\bar{p}_V$
1/10 ($k=1$)	24	2.25966		2.77614	
1/20 ($k=2$)	48	2.04967	2.31207	1.78156	2.63645
1/40 ($k=3$)	96	2.00690	2.05912	2.01079	2.05942
1/80 ($k=4$)	192	2.00062	2.00598	2.00569	2.01213

variables, as desired. Furthermore, we tested what would happen if we interpolate f, in the manner described as the end of Section 3.3; the results are given in Table 6, which shows that p and $\bar{p}$ both converged to 2—a significant finding, since it indicates that the method should prove reliable even if there is no closed-form expression for f^*.

A remaining loose end is why we have managed to obtain $p=2$ for all variables in Tables 5 and 6, even though inequality (88) is not satisfied on the finest mesh. The reason appears to be that the equation being solved—Eq.(26)—contains $\tau\exp(-a\tau\eta)$ rather than just $\exp(-a\tau\eta)$; consequently, as $\Delta\tau$ is decreased, the size of this source term decreases. It is evident that the largest value that this term can take—and hence which the method neglects, because of the finiteness of the computational domain—occurs when $\tau=1/a\eta_\infty$ and is equal to $e^{-1}/a\eta_\infty$. Thus, in Tables 5 and 6, this appears to be small enough to ensure that p and $\bar{p}$ still both converge to 2. As a corollary, we can note this as being a further positive side effect of using similarity-like variables rather than the original physical variables, even though the problem does not actually have a similarity solution.

5. CONCLUSIONS

This article has considered the effect of discontinuous boundary conditions on the accuracy of the Keller box finite-difference method for parabolic PDEs. Via a detailed study of four particular cases involving the linear 1-D transient heat equation, for which there were analytical solutions, we have established a systematic methodology for handling discontinuities in either the temperature or the heat flux. In particular, it was found that the scheme, which is second-order-accurate when there are no discontinuities, can lose numerical accuracy if due care is not taken through the choice of appropriate dependent and independent variables for numerical integration. For example, if the temperature and heat flux, T and T_x, respectively, are both continuous at the boundary, then T_x is still only first-order-accurate; however, by identifying the appropriate similarity-like variables, it was possible to reformulate the problem in a way that gave second-order accuracy for both T and T_x.

There are a number of ways in which these results can be used. First of all, the benchmark problems that were considered should provide guidance in the numerical solution of nonlinear parabolic PDEs for which there are no closed-form analytical solutions. Furthermore, the analysis presented will assist in the formulation of second-order-accurate numerical schemes for moving-boundary (Stefan) problems in continuous casting and ablation, in which the time for onset of phase change, corresponding

to a discontinuous boundary condition, is *a priori* unknown [7–9]; in this context, our method should compete well against other ones for Stefan problems that have recently been derived [20, 21].

REFERENCES

1. A. J. V. de Vooren and D. Djikstra, The Navier-Stokes Solution for Laminar Flow Past a Semi-infinite Plate, *J. Eng. Math.*, vol. 4, pp. 9–27, 1970.
2. F. T. Smith, Boundary-Layer Flow Near a Discontinuity in Wall Conditions, *J. Inst. Math. Appl.*, vol. 13, pp. 127–145, 1974.
3. A. E. P. Veldman, A New Calculation of the Wake of a Plate, *J. Eng. Math.*, vol. 9, pp. 65–70, 1975.
4. T. Cebeci, F. Thiele, P. G. Williams, and K. Stewartson, On the Calculation of Symmetric Wakes. I. Two-Dimensional Flows, *Num. Heat Transfer*, vol. 2, pp. 35–60, 1979.
5. M. Vynnycky, Concerning Closed-Streamline Flows with Discontinuous Boundary Conditions, *J. Eng. Math.*, vol. 33, pp. 141–156, 1998.
6. G. K. Batchelor, On Steady Laminar Flow with Closed Streamlines at Large Reynolds Number, *J. Fluid Mech.*, vol. 1, pp. 177–190, 1956.
7. J. Åberg, M. Vynnycky, and H. Fredriksson, Heat-Flux Measurements of Industrial On-Site Continuous Copper Casting and Their Use as Boundary Conditions for Numerical Simulations, *Trans. Ind. Inst. Metals*, vol. 62, pp. 443–446, 2009.
8. M. Vynnycky, A Mathematical Model for Air-Gap Formation in Vertical Continuous Casting: The Effect of Superheat, *Trans. Ind. Inst. Metals*, vol. 62, pp. 495–498, 2009.
9. S. L. Mitchell, and M. Vynnycky, An Accurate Finite-Difference Method for Ablation-Type Problems, *J. Comput. Appl. Math.*, vol. 236, pp. 4181–4192, 2012.
10. M. Vynnycky and N. Ipek, Reaction-Layer Asymptotics and the Electrochemical Pickling of Steel, *Proc. R. Soc. A*, vol. 467, pp. 2534–2560, 2011.
11. M. Vynnycky and K. I. Borg, On the Application of Concentrated Solution Theory to the Forced Convective Flow of Excess Supporting Electrolyte, *Electrochim. Acta*, vol. 55, pp. 7109–7117, 2010.
12. M. Vynnycky and N. Ipek, Supporting Electrolyte Asymptotics and the Electrochemical Pickling of Steel, *Proc. R. Soc. A*, vol. 465, pp. 3771–3797, 2009.
13. J. C. Strikwerda, *Finite Difference Schemes and Partial Differential Equations*, 2nd ed., Society for Industrial Mathematics, Philadelphia, PA, 2004.
14. T. Cebeci and P. Bradshaw, *Momentum Transfer in Boundary Layers*, Hemisphere, Washington, DC, 1977.
15. T. Cebeci and P. Bradshaw, *Physical and Computational Aspects of Convective Heat Transfer*, Springer-Verlag, New York, NY, 1984.
16. T. Cebeci and J. Cousteix, *Modeling and Computation of Boundary-Layer Flows*, Horizons Publishing Inc., CA, 2005.
17. S. L. Mitchell and M. Vynnycky, Finite-Difference Methods with Increased Accuracy and Correct Initialization for One-Dimensional Stefan Problems, *Appl. Math. Comput.*, vol. 215, pp. 1609–1621, 2009.
18. S. L. Mitchell, M. Vynnycky, I. G. Gusev, and S. S. Sazhin, An Accurate Numerical Solution for the Transient Heating of An Evaporating Droplet, *Appl. Math. Comput.*, vol. 217, pp. 9219–9233, 2011.
19. M. Vynnycky and S. L. Mitchell, On the Solution of Stefan Problems with Delayed Onset of Phase Change, *Proc. 7th HEFAT Conference*, Antalya, Turkey, pp. 709–714, 2010 (CD-ROM).

20. A. Ayasoufi, R. K. Rahmani, and T. G. Keith, Stefan Number-Insensitive Numerical Simulation of the Enthalpy Method for Stefan Problems Using the Space-Time CE/SE Method, *Numer. Heat Transfer., B*, vol. 55, pp. 257–272, 2009.
21. D. Slota, Homotopy Perturbation Method for Solving the Two-Phase Inverse Stefan Problem, *Numer. Heat Transfer., A*, vol. 59, pp. 755–768, 2011.